Ultra-strong attosecond laser focus produced by a relativistic-flying parabolic mirror

Tae Moon Jeong*[a], Sergei V. Bulanov[a,b], Petr Valenta[a,c], Georg Korn[a], Timur Zh. Esirkepov[b], James K. Koga[b], and Alexander S. Pirozhkov[b]
[a]Institute of Physics of the ASCR, ELI-Beamlines, Na Slovance 2, 18221 Prague, Czech Republic;
[b]Kansai Photon Science Institute, National Institutes for Quantum and Radiological Science and Technology, 8-1-7 Umemidai, Kizugawa-shi, Kyoto 619-0215, Japan;
[c]Faculty of Nuclear Sciences and Physical Engineering, Czech Technical University in Prague, Brehova 7, 11519 Prague, Czech Republic

ABSTRACT

The reflection of a laser pulse by a relativistic-moving mirror is one of fundamental problems encountered in the high-power laser and plasma interactions. It is well known that a laser pulse reflected by a relativistic-flying mirror experiences the intensification of its intensity, frequency up-shift, and shortening of pulse duration. Thus, it is of fundamental interest to have a mathematical solution expressing the intensity distribution of a laser pulse reflected by a relativistic-flying parabolic mirror. In this paper, we present analytical and mathematical formulae describing the electromagnetic field of a laser pulse reflected and focused by the relativistic-flying parabolic mirror.

Keywords: relativistic-flying mirror, attosecond laser pulse, 4π-spherical focusing, cylindrical vector beam

1. INTRODUCTION

The relativistic-flying mirror (RFM) is one of the well-known plasma optics observed when an intense laser pulse propagates through an under-dense plasma medium. A laser pulse reflected by the RFM experiences the enhancement in field strength and the up-shift of angular frequency due to the Lorentz γ-factor of the RFM [1]. Owing to the frequency up-shift property of the RFM, the RFM is considered as a highly promising candidate for generating atto-second light sources in the x-ray range. The RFM is a high-density electron layer and a part of the plasma cavity formed behind a propagating laser pulse. The physical properties of a laser pulse reflected by the RFM can be found in recent publications [2-7]. The RFM formed in the plasma cavity can be understood as a relativistic-flying parabolic mirror (RFPM) due to its paraboloidal shape. Typically, the focus of the RFPM is short, and the relativistic motion of the RFPM makes the focal length even shorter in the boosted frame of reference. As a result of relativistic motion and short focal length, the laser field distribution reflected and focused by the RFPM becomes very complicated, and mathematical formulae describing the electromagnetic field distribution of a laser pulse focused by a RFPM is of fundamental interest.

In this paper, we show that the electromagnetic field distribution focused by the RFPM can be analytically calculated for a cylindrical vector (radially-polarized and azimuthally-polarized) beam [8,9] through the Lorentz transformation-Diffraction integral-Lorentz transformation (LDL) approach. In this approach, an incident radially-polarized (or azimuthally-polarized) laser pulse in the laboratory frame of reference is first Lorentz-transformed into the boosted frame of reference, in which the RFPM is at rest. Since the f-number << 1 in the boosted frame of reference, the focused field distribution is calculated by the diffraction integral under the 4π-spherical focusing condition [10]. The 4π-spherical focusing scheme was proposed to maximize the intensity of a laser pulse with a given laser power and it is applied to investigate quantum electrodynamic phenomena under ultra-strong laser intensity [10,11]. The focused field distribution obtained in the boosted frame of reference is then Lorentz-transformed to the laboratory frame of reference. The field enhancement, frequency up-shift, and the pulse duration change of a laser pulse focused by the RFPM are examined from the mathematical formulae obtained.

*taemoon.jeong@eli-beams.eu; phone +420 266 051 551; eli-beams.eu

International Conference on X-Ray Lasers 2020, edited by Davide Bleiner,
Proc. of SPIE Vol. 11886, 118860H · © 2021 SPIE · CCC code:
0277-786X/21/$21 · doi: 10.1117/12.2592047

2. FORMATION OF ELECTROMAGNETIC FIELD UNDER 4Π-SPHERICAL FOCUSING SCHEME

In this section, we briefly show how to calculate the focused electromagnetic field through the diffraction integral in the boosted frame of reference. According to ref. [3], the focal length of the RFPM becomes shortened in the boosted frame of reference (expressed as the moving frame in [3]). The shortening of the focal length changes the focusing condition for the RFPM to the 4π-spherical focusing condition. The 4π-spherical focusing scheme can be regarded as an extreme case of the tight focusing scheme. And, it is known that a focused intensity of ~10^{27} W/cm^2 is possible by 4π-spherically focusing a 100 PW laser pulse with a wavelength of 0.2 μm [11]. By applying the diffraction integral, the electric field at an observation position located near to the focus in the boosted frame of reference can be calculated by,

$$d\vec{E}'_O\left(\rho'_O,\theta'_O,\phi'_O\right)=\frac{ik'}{2\pi}\vec{E}'_S\left(\theta'_S,\phi'_S\right)\frac{\exp\left(i\vec{k}'\cdot\vec{u}'\right)}{\left|\vec{u}'\right|}dA'. \tag{1}$$

The prime is used to represent coordinates and variables in the boosted frame of reference. Thus, the spherical coordinates, $\left(\rho'_O,\theta'_O,\phi'_O\right)$ and the electric field, $E'_S\left(\theta'_S,\phi'_S\right)$, mean the observation point and the electric field at a source point $\left(\rho'_S,\theta'_S,\phi'_S\right)$ on a virtual focusing sphere in the boosted frame of reference. dA' is the infinitesimal area of the source point. The electric fields for the radially-polarized (transverse magnetic, TM) and the azimuthally-polarized (transverse electric, TE) waves are expressed as

$$\vec{E}'_{TM}\left(k'\right)=ik'\mathcal{A}\left(k'\right)\frac{\sin\left(k'\rho'\right)}{k'\rho'}\sin\theta'\exp\left(-i\omega't'\right)\hat{\theta}', \text{ and } \vec{E}'_{TE}\left(k'\right)=ik'\mathcal{A}\left(k'\right)\frac{\sin\left(k'\rho'\right)}{k'\rho'}\sin\theta'\exp\left(-i\omega't'\right)\hat{\phi}'. \tag{2}$$

Here, $\mathcal{A}\left(k'\right)$ is the field strength at a wavenumber of k' ($=\omega'/c$). By introducing a proper beam shaper to the electromagnetic wave, the electric field on the virtual focusing sphere can be written by

$$E'_S\left(\theta'_S,\phi'\right)=E'_S\sin\theta'_S. \tag{3}$$

Now, by inserting eq. (3) into eq. (1), the resultant expression for the electric field at the observation point is expressed as

$$\vec{E}'_O=\hat{\theta}'\frac{ik'\rho'_S}{2\pi}E'_S\exp\left(ik'\rho'_S\right)\int\exp\left(-ik'r'_O\cos\zeta\right)\sin^2\theta'_S d\theta'_S d\phi'_S. \tag{4}$$

Here, ζ is the angle between two vectors to the source and the observation points from the origin, and $\cos\zeta$ can be explicitly expressed as $\cos\theta'_S\cos\theta'_O\cos\left(\phi'_S-\phi'_O\right)+\sin\theta'_S\sin\theta'_O$.

The integration of eq. (4) yields the electric field distribution near the focus in the boosted frame of reference. Then, the focused electric field for the TM mode electromagnetic wave is given by,

$$\vec{E}'_{O,TM}=\hat{\theta}'iE'_p\exp\left(ik'\rho'_S\right)S_a\left(\rho'_O,\theta'_O\right). \tag{5}$$

where the spatial distribution function, $S_a\left(\rho'_O,\theta'_O\right)$, is defined as

$$S_a\left(\rho'_O,\theta'_O\right)=\left[j_0\left(k'\rho'_O\right)+\frac{5}{2^3}j_2\left(k'\rho'_O\right)P_2\left(\cos\theta'_O\right)-\frac{9}{2^6}j_4\left(k'\rho'_O\right)P_4\left(\cos\theta'_O\right)+\cdots\right]. \tag{6}$$

The focused electric field distribution for the TE mode electromagnetic wave in the focal region is calculated as,

$$\vec{E}'_{O,TE}=-\hat{\phi}'E'_P\exp\left(ik'\rho'_S\right)S_b\left(\rho'_O,\theta'_O\right), \tag{7}$$

where another spatial distribution function, $S_b\left(\rho'_O,\theta'_O\right)$, is defined as

$$S_b\left(\rho'_O,\theta'_O\right)=\frac{4}{\pi}j_1\left(k'\rho'_O\right)P_1^1\left(\cos\theta'_O\right). \tag{8}$$

Due to the symmetric property of the polarization, the magnetic field of the TM mode electromagnetic field has the same field configuration as the electric field of the TE mode electromagnetic field, and vice versa. By using the symmetric property, the magnetic fields for TM and TE mode electromagnetic waves are given by

$$\vec{H}'_{O,TM}=-\hat{\phi}'H'_P\exp\left(ik'\rho'_S\right)S_b\left(\rho'_O,\theta'_O\right),\ \text{and}\ \vec{H}'_{O,TE}=\hat{\theta}'iH'_p\exp\left(ik'\rho'_S\right)S_a\left(\rho'_O,\theta'_O\right). \tag{9}$$

The electric and magnetic field distributions for the TM mode electromagnetic wave are shown in Fig. 1(a). The first zeros of the field strength appear at ~ 0.6 λ in both x/y-axis and z-axis. Figure 1(b) shows the line-out data of the electric field along the z'-direction. Different-colored lines in the figure refer to the field profile calculated by summing up different orders of the spherical Bessel function. Summing up the higher order terms of the spherical Bessel function shows a better confinement of the field in space.

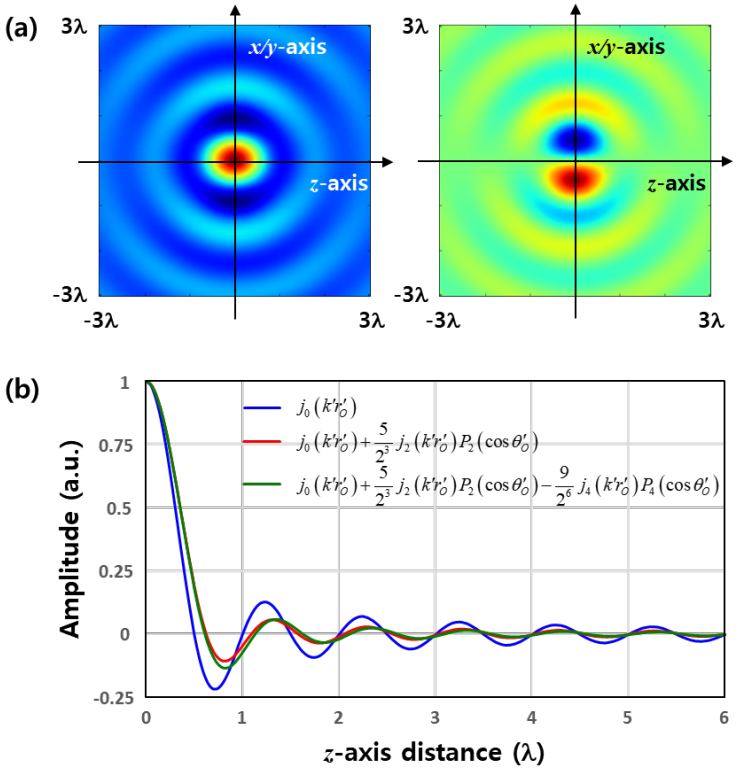

Figure 1. (a) Electric and magnetic field distributions of a radially-polarized electromagnetic field focused under the 4π-spherical focusing scheme in the boosted frame of reference. Red color refers to the positive field and blue to the negative field. (b) Line-out profiles of the electric field distributions along the z-direction. Different colors refer to the line profile obtained by summing up different higher order terms.

3. ELECTROMAGNETIC FIELD OF LASER PULSE FOCUSED BY A RELATIVISTIC-FLYING PARABOLIC MIRROR

In the previous section, we calculated the focused field distribution in the boosted frame of reference for the monochromatic wave. A laser pulse is formed by the superposition of monochromatic components in the laser spectrum. An incident laser pulse with a Gaussian distribution, $G(\omega)=e^{-(\omega-\omega_0)^2/(\Delta\omega)^2}$, (of which a center frequency and a bandwidth are given by ω_0 and $\Delta\omega$, respectively) in the ω-space is assumed, and it is calculated in a laboratory frame of reference through the Fourier transformation as,

$$E(t)=E_0(x,y)\int_{-\infty}^{\infty}G(\omega)e^{i\omega(t+z/c)}d\omega=E_p\exp\left[-\frac{1}{\Delta t^2}(t+z/c)^2\right]e^{i\omega_0(t+z/c)}. \tag{10}$$

Here, $E_0(x,y)$ can be understood as the Laguerre-Gaussian function [$E\sim LG_0^1\sim(\rho/\rho_0)\exp(-\rho^2/2\rho_0^2)$] since the beam profile for the cylindrical vector beam (radially-polarized or azimuthally-polarized beam) follows the Laguerre-Gaussian function. The peak field strength, E_p, in time is $\sqrt{\pi}\Delta\omega E_0(x,y)$ and the pulse duration, Δt, $\sqrt{2}/\Delta\omega$.

Since the incident laser pulse propagates along the -z-axis ($\vec{k}=-k\hat{z}=-\omega/c\,\hat{z}$) and the RFPM moves at a speed of v along the +z-axis, the Lorentz transformations between the laboratory frame (unprimed coordinates) of reference to the boosted frame (primed coordinates) of reference are given by

$$ct=\gamma(ct'+\beta z'),\ x=x',\ y=y', \text{ and } z=\gamma(z'+\beta ct'), \text{ (for coordinates)} \tag{11-1}$$

$$\vec{E}_{0,\perp}=\gamma\left[\vec{E}'_{0,\perp}-c\vec{\beta}\times\vec{B}'_0\right] \text{ and } \vec{E}_{0,\parallel}=\vec{E}'_{0,\parallel}. \text{(for fields)} \tag{11-2}$$

Here, β and γ are defined as v/c and $1/\sqrt{1-\beta^2}$, respectively. The subscripts, $\perp$ and $\parallel$, mean the perpendicular and parallel polarization components of the field to the mirror moving direction. Then, the electric field in the boosted frame of reference is expressed as

$$E'(t')=E'_0(x',y')\int_{-\infty}^{\infty}G(\omega)e^{i\sqrt{(1+\beta)/(1-\beta)}\omega(t'+z'/c)}d\omega. \tag{12}$$

By introducing a new angular frequency, ω', in the boosted frame of reference as $\omega\sqrt{(1+\beta)/(1-\beta)}$ and performing the integration in the ω'-space, we obtain the electric field expression for the incident laser pulse in the boosted frame of reference as

$$E'(t')=E'_p\exp\left[-(t'+z'/c)^2/(\Delta t')^2\right]\exp\left[i\omega'_0(t'+z'/c)\right]. \tag{13}$$

with relationships of $E'_p=E_p\sqrt{(1+\beta)/(1-\beta)}$ and $\Delta t'=\Delta t\sqrt{(1-\beta)/(1+\beta)}$. In the relativistic limit ($\beta\to1$), it can be easily found that $\omega'_0\approx2\gamma\omega_0$, $\Delta\omega'\approx2\gamma\Delta\omega$, $E'_p\approx2\gamma E_p$, $\Delta t'=\Delta t/2\gamma$. This is the first Lorentz transformation taken when calculating the field distribution of a laser pulse focused by the RFPM. The first Lorentz transformation provides a new angular frequency and field strength in the boosted frame of reference for the following calculation.

After the first Lorentz transformation, the electric field strength is modified as $E'_p=E_p\sqrt{(1+\beta)/(1-\beta)}$, and the center frequency and the bandwidth are expressed by $\omega_0\sqrt{(1+\beta)/(1-\beta)}$ and $\Delta\omega\sqrt{(1+\beta)/(1-\beta)}$ in the boosted frame of reference. We calculate the diffraction integral with these new parameters. As shown in Sec. 2, the electromagnetic field distributions of the 4π-spherically focused monochromatic TM mode electromagnetic wave are expressed as,

$$\vec{E}'_f(x'^{\mu};\omega')=\hat{\theta}'iE'_{0,f}(\omega')S_a(\rho',\theta';\omega')\exp(-i\omega't')=\vec{E}'_{\perp,f}+\vec{E}'_{\parallel,f}, \tag{14-1}$$

$$\vec{H}'_f(x'^{\mu};\omega')=-\hat{\phi}'H'_{0,f}(\omega')S_b(\rho',\theta';\omega')\exp(-i\omega't')=\vec{H}'_{\parallel,f}. \tag{14-2}$$

In this case, the Gaussian distribution function, $G(\omega')$, in the boosted frame of reference is modified as $e^{-(\omega'-\omega'_0)^2/(\Delta\omega')^2}$. The spatiotemporal distribution of the electromagnetic fields of a laser pulse focused by a RFPM in the laboratory frame of reference can be obtained through the second Lorentz transformation from the boosted frame of reference to the laboratory frame of reference and a Fourier transformation in the frequency domain. After the Lorentz transformation for the field, we have the resultant field expressions in Cartesian coordinates as

$$E''_{f,x}\left(x'^{\mu};t'\right)=\int_{-\infty}^{\infty}E''_{f,x}\left(x'^{\mu};\omega'\right)\exp\left(i\omega't'\right)d\omega'=\gamma\left[iI_{Sa}\left(x'^{\mu};t'\right)\cos\theta'+\beta I_{Sb}\left(x'^{\mu};t'\right)\right]\cos\phi', \tag{15-1}$$

$$E''_{f,y}\left(x'^{\mu};t'\right)=\int_{-\infty}^{\infty}E''_{f,y}\left(x'^{\mu};\omega'\right)\exp\left(i\omega't'\right)d\omega'=\gamma\left[iI_{Sa}\left(x'^{\mu};t'\right)\cos\theta'+\beta I_{Sb}\left(x'^{\mu};t'\right)\right]\sin\phi', \tag{15-2}$$

$$E''_{f,z}\left(x'^{\mu};t'\right)=\int_{-\infty}^{\infty}E''_{f,z}\left(x'^{\mu};\omega'\right)\exp\left(i\omega't'\right)d\omega'=-iI_{Sa}\left(x'^{\mu};t'\right)\sin\theta', \tag{15-3}$$

$$H''_{f,x}\left(x'^{\mu};t'\right)=\int_{-\infty}^{\infty}H''_{f,x}\left(x'^{\mu};\omega'\right)\exp\left(i\omega't'\right)d\omega'=-\left(\gamma/c\right)\left[I_{Sb}\left(x'^{\mu};t'\right)+i\beta I_{Sa}\left(x'^{\mu};t'\right)\cos\theta'\right]\sin\phi', \tag{15-4}$$

$$H''_{f,y}\left(x'^{\mu};t'\right)=\int_{-\infty}^{\infty}H''_{f,y}\left(x'^{\mu};\omega'\right)\exp\left(i\omega't'\right)d\omega'=\left(\gamma/c\right)\left[I_{Sb}\left(x'^{\mu};t'\right)+i\beta I_{Sa}\left(x'^{\mu};t'\right)\cos\theta'\right]\cos\phi', \tag{15-5}$$

$$H''_{f,z}\left(x'^{\mu};t'\right)=\int_{-\infty}^{\infty}H''_{f,z}\left(x'^{\mu};\omega'\right)\exp\left(i\omega't'\right)d\omega'=0. \tag{15-6}$$

where $I_{Sa}\left(x'^{\mu};t'\right)$ and $I_{Sb}\left(x'^{\mu};t'\right)$ are definite integrals defined as

$$I_{Sa}\left(x'^{\mu};t'\right)=\frac{cE'_{c,f}}{2i\rho'}\int_{-\infty}^{\infty}G\left(\omega'\right)S_a\left(\rho',\theta';\omega'\right)\exp\left(i\omega't'\right)d\omega', \tag{16-1}$$

$$I_{Sb}\left(x'^{\mu};t'\right)=\frac{cE'_{c,f}}{2i\rho'}\int_{-\infty}^{\infty}G\left(\omega'\right)S_b\left(\rho',\theta';\omega'\right)\exp\left(i\omega't'\right)d\omega'. \tag{16-2}$$

The subscripts *x*, *y*, and *z* refer to the x-, y-, z-polarization components. In eqs. (15) and (16), the fields are Lorentz-transformed from the boosted frame of reference to the laboratory frame of reference, but the coordinates have not yet been transformed. The spatial distribution functions, $S_a\left(\rho',\theta';\omega'\right)$ and $S_b\left(\rho',\theta';\omega'\right)$, contain spherical Bessel functions, and the spherical Bessel function contains the in-coming [$\exp\left(i\,\omega'\rho'/c\right)$] and the out-going [$\exp\left(-i\,\omega'\rho'/c\right)$] field components. The Lorentz invariant property of the phase for the in-coming ($\omega't'+\omega'\rho'/c$) wave is expressed by

$$\begin{aligned}\omega't'+\omega'\rho'/c&=\omega't\gamma\left(1-\beta\cos\theta'\right)+k'x\sin\theta'\cos\phi'+k'y\sin\theta'\sin\phi'+k'z\gamma\left(\cos\theta'-\beta\right)\\&=\omega t+kx\sin\theta\cos\phi+ky\sin\theta\sin\phi+kz\cos\theta\\&=\omega t+\omega\rho/c.\end{aligned} \tag{17}$$

Here, the unprimed quantities are coordinates (*x*, *y*, and *z*), angles (θ and ϕ), and wavenumber (*k*) in the laboratory frame of reference. The azimuthal angle, ϕ', is not affected by the Lorentz transformation, so $\phi'=\phi$. From eq. (17), we obtain the Lorentz transformation properties for the angular frequency and the wavevector of the in-coming wave as,

$$\omega=\omega'\gamma\left(1-\beta\cos\theta'\right),\ \ k'\sin\theta'=k\sin\theta,\ \text{and}\ \ k'\gamma\left(\cos\theta'-\beta\right)=k\cos\theta. \tag{18}$$

And the relationship between polar angles in the laboratory and boosted frame of references are given as

$$\sin\theta'=\frac{\sin\theta}{\gamma\left(1+\beta\cos\theta\right)},\ \text{and}\ \cos\theta'=\frac{\cos\theta+\beta}{1+\beta\cos\theta}. \tag{19}$$

The Lorentz invariant property of the phase for the out-going ($\omega't'-\omega'\rho'/c$) wave is expressed by

$$\begin{aligned}\omega't'-\omega'\rho'/c&=\omega't\gamma\left(1+\beta\cos\theta'\right)-k'x\sin\theta'\cos\phi'-k'y\sin\theta'\sin\phi'-k'z\gamma\left(\cos\theta'+\beta\right)\\&=\omega t-kx\sin\theta\cos\phi-ky\sin\theta\sin\phi-kz\cos\theta\\&=\omega t-\omega\rho/c.\end{aligned} \tag{20}$$

Similarly, we obtain the Lorentz transformation properties for the angular frequency and the wavevector of the out-going wave as,

$$\omega = \omega'\gamma\left(1+\beta\cos\theta'\right),\ \ k'\sin\theta' = k\sin\theta,\ \text{and}\ \ k'\gamma\left(\cos\theta'+\beta\right) = k\cos\theta. \tag{21}$$

And, the relationship between polar angles in the laboratory and boosted frame of references are given as

$$\sin\theta' = \frac{\sin\theta}{\gamma\left(1-\beta\cos\theta\right)},\ \text{and}\ \cos\theta' = \frac{\cos\theta-\beta}{1-\beta\cos\theta}. \tag{22}$$

Now, after dividing $I_{Sa}\left(x'^{\mu};t'\right)\cos\theta'$ and $I_{Sb}\left(x'^{\mu};t'\right)$ into two parts (in-coming and out-going field parts) and performing the integration, we finally derive the mathematical expressions for the spatiotemporal distribution of the electromagnetic field in the laboratory frame of reference as,

$$\begin{aligned} E''_{f,x}\left(\rho,\theta;t\right) = -\gamma\sqrt{\frac{1+\beta}{1-\beta}}\frac{\pi\omega'_0\Delta\omega'}{4}\sqrt{\frac{3A_{eff}\mathcal{I}}{c\varepsilon_0}}\Bigg\{ & j_0\left[\frac{\omega'_0}{c}R\left(\rho,t\right)\right]\sin\left[\omega'_0T\left(t,\rho\right)\right]\Upsilon_{\cos\theta'}\left(T,R\right) \\ & -\beta j_1\left[\frac{\omega'_0}{c}R\left(\rho,t\right)\right]\cos\left[\omega'_0T\left(t,\rho\right)\right]\Upsilon_{\sin\theta'}\left(T,R\right)\Bigg\}\cos\phi, \end{aligned} \tag{23-1}$$

$$\begin{aligned} E''_{f,y}\left(\rho,\theta;t\right) = -\gamma\sqrt{\frac{1+\beta}{1-\beta}}\frac{\pi\omega'_0\Delta\omega'}{4}\sqrt{\frac{3A_{eff}\mathcal{I}}{c\varepsilon_0}}\Bigg\{ & j_0\left[\frac{\omega'_0}{c}R\left(\rho,t\right)\right]\sin\left[\omega'_0T\left(t,\rho\right)\right]\Upsilon_{\cos\theta'}\left(T,R\right) \\ & -\beta j_1\left[\frac{\omega'_0}{c}R\left(\rho,t\right)\right]\cos\left[\omega'_0T\left(t,\rho\right)\right]\Upsilon_{\sin\theta'}\left(T,R\right)\Bigg\}\sin\phi, \end{aligned} \tag{23-2}$$

$$E''_{f,z}\left(\rho,\theta;t\right) = \sqrt{\frac{1+\beta}{1-\beta}}\frac{\pi\omega'_0\Delta\omega'}{4}\sqrt{\frac{3A_{eff}\mathcal{I}}{c\varepsilon_0}}j_0\left[\frac{\omega'_0}{c}R\left(\rho,t\right)\right]\sin\left[\omega'_0T\left(t,\rho\right)\right]\Upsilon_{\sin\theta'}\left(T,R\right), \tag{23-3}$$

$$\begin{aligned} H''_{f,x}\left(\rho,\theta;t\right) = -\gamma\sqrt{\frac{1+\beta}{1-\beta}}\frac{\pi\Delta\omega'\omega'_0}{4c}\sqrt{\frac{3A_{eff}\mathcal{I}}{c\varepsilon_0}}\Bigg\{ & j_1\left[\frac{\omega'_0}{c}R\left(\rho,t\right)\right]\cos\left[\omega'_0T\left(t,\rho\right)\right]\Upsilon_{\sin\theta'}\left(T,R\right) \\ & -\beta j_0\left[\frac{\omega'_0}{c}R\left(\rho,t\right)\right]\sin\left[\omega'_0T\left(t,\rho\right)\right]\Upsilon_{\cos\theta'}\left(T,R\right)\Bigg\}\sin\phi, \end{aligned} \tag{23-4}$$

$$\begin{aligned} H''_{f,y}\left(\rho,\theta;t\right) = \gamma\sqrt{\frac{1+\beta}{1-\beta}}\frac{\pi\Delta\omega'\omega'_0}{4c}\sqrt{\frac{3A_{eff}\mathcal{I}}{c\varepsilon_0}}\Bigg\{ & j_1\left[\frac{\omega'_0}{c}R\left(\rho,t\right)\right]\cos\left[\omega'_0T\left(t,\rho\right)\right]\Upsilon_{\sin\theta'}\left(T,R\right) \\ & -\beta j_0\left[\frac{\omega'_0}{c}R\left(\rho,t\right)\right]\sin\left[\omega'_0T\left(t,\rho\right)\right]\Upsilon_{\cos\theta'}\left(T,R\right)\Bigg\}\cos\phi, \end{aligned} \tag{23-5}$$

$$H''_{f,z}\left(\rho,\theta;t\right) = 0. \tag{23-6}$$

Here, $\mathcal{I}$ is the intensity of the incident laser pulse and A_{eff} the effective area of the incident laser. The envelope functions, $\Upsilon_{\cos\theta'}\left(T,R\right)$ and $\Upsilon_{\sin\theta'}\left(T,R\right)$, are defined as

$$\Upsilon_{\cos\theta'}\left(T,R\right) = \frac{1}{2}\left\{\frac{\cos\theta+\beta}{1+\beta\cos\theta}\exp\left[-\frac{\left(\Delta\omega'\right)^2}{4}\left(T+\frac{R}{c}\right)^2\right]+\frac{\cos\theta-\beta}{1-\beta\cos\theta}\exp\left[-\frac{\left(\Delta\omega'\right)^2}{4}\left(T-\frac{R}{c}\right)^2\right]\right\}, \tag{24-1}$$

$$\Upsilon_{\sin\theta'}\left(T,R\right) = \frac{1}{2}\left\{\frac{\sin\theta}{\gamma\left(1+\beta\cos\theta\right)}\exp\left[-\frac{\left(\Delta\omega'\right)^2}{4}\left(T+\frac{R}{c}\right)^2\right]+\frac{\sin\theta}{\gamma\left(1-\beta\cos\theta\right)}\exp\left[-\frac{\left(\Delta\omega'\right)^2}{4}\left(T-\frac{R}{c}\right)^2\right]\right\}. \tag{24-2}$$

The new variables, $T(t,\rho)$ and $R(\rho,t)$, used in eqs. (23) and (24) are functions of t and ρ, and given by

$$T(t,\rho)=\frac{t-(\rho/c)\beta\cos\theta}{\gamma\left(1-\beta^2\cos^2\theta\right)} \text{ and } R(\rho,t)=\frac{\rho-ct\beta\cos\theta}{\gamma\left(1-\beta^2\cos^2\theta\right)}. \tag{25}$$

Equation (23) provides information on how the field of the electromagnetic pulse focused by the RFPM is distributed in the space and time domain. The nominal pulse duration is determined by the argument of exponential function in the envelope function. From eq. (24), the nominal pulse duration reflected and focused by the RFPM is calculated as $\left(\sqrt{2}/\Delta\omega\right)\frac{1-\beta\cos\theta}{1+\beta}$ in the laboratory frame of reference. Since $\omega_0'=\omega_0\sqrt{\frac{1+\beta}{1-\beta}}$ and $\Delta\omega'=\Delta\omega\sqrt{\frac{1+\beta}{1-\beta}}$, the field strength for the perpendicular polarization component is proportional to $\gamma\left(\frac{1+\beta}{1-\beta}\right)^{3/2}\mathcal{I}^{0.5}$ as shown in eq. (23) and in the relativistic limit it becomes proportional to $8\gamma^4\mathcal{I}^{0.5}$. The parallel polarization component becomes relatively weaker than the perpendicular ones in the relativistic limit. The phase is given by $\omega_0'T\pm\omega_0'\frac{R}{c}$ for the in-coming (+) or out-going (-) field, and by using eq. (25) we have the phase as $\frac{1+\beta}{1\pm\beta\cos\theta}\omega_0\left(t\pm\frac{\rho}{c}\right)$ in the laboratory frame of reference. Thus, the angular frequency is enhanced by a factor of $(1+\beta)/(1\pm\beta\cos\theta)$.

4. CONCLUSION

The relativistic-flying mirror is a promising candidate for generating attosecond intense electromagnetic pulses. The analytic formulae describing the three-dimensional electromagnetic field distribution of a laser pulse focused by a relativistic-flying parabolic mirror are derived through the Lorentz transformation-Diffraction integral-Lorentz transformation (LDL) approach. From the calculation with the radially-polarized electromagnetic pulse, the field strength is enhanced by a factor of $\sim\gamma^4$ in the relativistic limit. In this study, we assume an ideal parabolic mirror with perfect reflection. In a realistic situation, the reflection depends on the incident angle to the parabolic surface and the polarization (p or s polarization). When considering the radially- or azimuthally-polarized laser pulse, the reflectance becomes dependent only on the incident angle to the parabolic surface. Therefore, the modification with a realistic reflectance depending on the incident angle will be another interesting topic to be considered.

ACKNOWLEDGEMENT

The work was supported by the project High Field Initiative (CZ.02.1.01/0.0/0.0/15_003/0000449) from the European Regional Development Fund.

REFERENCES

[1] Bulanov, S. V., Esirkepov, T., and Tajima, T., "Light Intensification towards the Schwinger Limit," Phys. Rev. Lett. 91, 085001 (2003).

[2] Bulanov, S. V., Esirkepov, T. Zh., Kando, M., Pirozhkov, A. S., and Rosanov, N. N., "Relativistic Mirrors in Plasmas–Novel Results and Perspectives," Physics Uspekhi 56, 429-464 (2013).

[3] Bulanov, S. V., Esirkepov, T. Zh., Kando, M., and Koga, J., "Relativistic mirrors in laser plasmas (analytical methods)," Plasma Sources Sci. Technol. 25, 053001 (2016).

[4] Koga, J. K., Bulanov, S. V., Esirkepov, T. Zh., Kando, M., Bulanov, S. S., and Pirozhkov, A. S., "Relativisitcally upshifted higher harmonic generation via relativistic flying mirrors," Plasma Phys. Control. Fusion 60, 074007 (2018).
[5] Valenta, P., Esirkepov, T. Zh., Koga, J. K., Pirozhkov, A. S., Kando, M., Kawachi, T., Liu, Y.-K., Fang, P., Chen, P., Mu, J., Korn, G., Klimo, O., and Bulanov, S. V., "Recoil effects on reflection from relativistic mirrors in laser plasmas," Phys. Plasma 27, 032109 (2020).
[6] Esirkepov, T. Zh., Mu, J., Gu, Y., Jeong, T. M., Valenta, P., Klimo, O., Koga, J. K., Kando, M., Neely, D., Korn, G., and Bulanov, S. V., "Optical probing of relativistic plasma singularities," Phys. Plasmas 27, 052103 (2020).
[7] Mu, J., Esirkepov, T. Zh., Valenta, P., Gu, Y., Jeong, T. M., Pirozhkov, A. S., Koga, J. K., Kando, M., Korn, G., and Bulanov, S. V., "Relativistic flying forcibly oscillating reflective diffraction grating," Phys. Rev. E 102, 053202 (2020).
[8] Jeong, T. M., Bulanov, S. V., Weber, S., and Korn, G., "Analysis on the longitudinal field strength formed by tightly-focused radially-polarized femtosecond petawatt laser pulse," Opt. Express 26, 33091 (2018).
[9] Jeong, T.M., Bulanov, S.V., Yan, W., Weber, S., and Korn, G., "Generation of superposition modes by polarization-phase coupling in a cylindrical vector orbital angular momentum beam," OSA Continuum 2, 2718 (2019).
[10] Jeong, T. M., Bulanov, S. V., Sasorov, P. V., Bulanov, S. S., Koga, J. K., and Korn, G., "4π-spherically focused electromagnetic wave: diffraction optics approach and high-power limits," Opt. Express 28, 13991 (2020).
[11] Jeong, T. M., Bulanov, S. V., Sasorov, P. V., Korn, G., Koga, J. K., and Bulanov, S. S., "Photon scattering by a 4π-spherically-focused ultrastrong electromagnetic wave," Phys. Rev. A 102, 023504 (2020).
[12] D. Bleiner, The Science and Technology of X-ray Lasers: A 2020 Update Proc. SPIE 11886, 1188602 (2021)